

Lewis Acid Catalyzed $[\text{RFe}(\text{CO})_4]^-$ Alkyl Migration Reactions. A Mechanistic Investigation

James P. Collman,*¹ Richard G. Finke, James N. Cawse, and John I. Brauman*¹

Contribution from the Department of Chemistry, Stanford University, Stanford, California 94305. Received January 9, 1978

Abstract: This paper is a kinetic and mechanistic study of alkyl migration reactions of $(\text{RFe}(\text{CO})_4)^-$. Catalysis of these reactions by Lewis acid ion pairing is discussed. The study includes analysis of the several types of ion pairs derived from $\text{NaRFe}(\text{CO})_4$ and $\text{NaRC}(\text{O})\text{Fe}(\text{CO})_4$ in THF and their interconnecting equilibrium constants, as well as IR and ^{13}C NMR evidence implicating the acyl group as the cation binding site in $(\text{RC}(\text{O})\text{Fe}(\text{CO})_4)^-$. The overall rate law is determined, and kinetic data are presented showing the effect of various cations and crown ether complexed cations as well as CO and a variety of phosphines. Solvent and temperature effects upon this reaction are also given. A mechanism for $(\text{RFe}(\text{CO})_4)^-$ alkyl migration reactions is discussed in light of previous studies of alkyl migration reactions.

There is increasing interest in the use of organotransition metal reagents in organic synthesis. Since 1970 much of our work in this area has been directed toward understanding the reactions of $\text{Na}_2\text{Fe}(\text{CO})_4$ and its organic derivatives. Previously, we described the use of $\text{Na}_2\text{Fe}(\text{CO})_4$ to convert alkyl halides or sulfonates into aldehydes,^{2a} unsymmetrical ketones,^{2b} carboxylic acids,^{2c} esters,^{2c} and amides^{2c} (Scheme I). The use of $\text{Na}_2\text{Fe}(\text{CO})_4$ for organic as well as inorganic synthesis has recently been reviewed.^{2d}

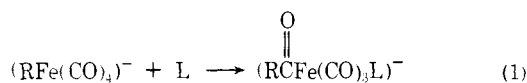
Central to these synthetic conversions is the alkyl migration "migratory insertion" reaction: $(\text{RFe}(\text{CO})_4)^- \rightarrow \text{RC}(\text{O})\text{Fe}(\text{CO})_3(\text{L})^-$, Scheme I). Such reactions have played an important and unifying role in organotransition metal chemistry. We have studied alkyl migration as well as many of the other reactions in Scheme I in some detail, with the hope that an understanding of the underlying mechanisms will promote practical applications of $\text{Na}_2\text{Fe}(\text{CO})_4$ and other organotransition metal reagents.

Early on, our interest in the mechanisms of the reactions in Scheme I was increased by the observation of dramatic ion-pairing effects on the oxidative-addition reactions of the super-nucleophile,⁴ $\text{Na}_2\text{Fe}(\text{CO})_4$, and on Lewis acid catalysis⁵ of alkyl migration reactions involving $(\text{RFe}(\text{CO})_4)^-$.

In this paper we present detailed kinetic and other mechanistic studies of alkyl migration reactions of $(\text{RFe}(\text{CO})_4)^-$. The nature of the ionic species (tight and solvent-separated ion pairs, triple ions, and dissociated ions) derived from $\text{NaRFe}(\text{CO})_4$ in THF along with their interconnecting equilibrium constants and relative reactivities has been determined. The relative rates of alkyl migration in the presence of CO and a series of phosphines, along with the relative migratory aptitudes of benzyl and *n*-alkyl groups, have been measured. Solvent effects and temperature parameters have also been determined.

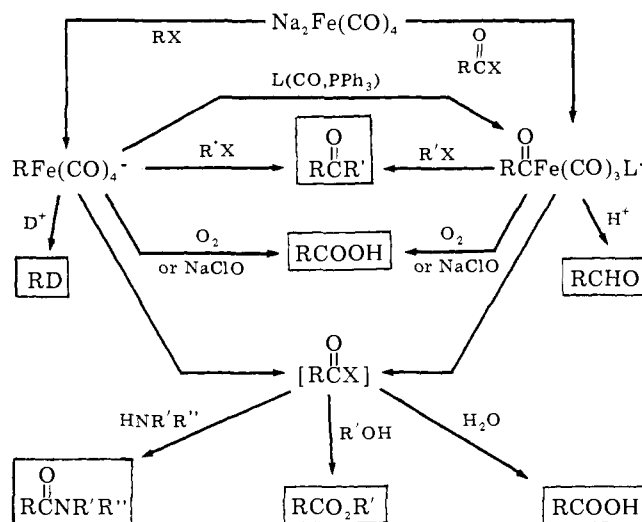
Results and Discussion

The reaction of interest is alkyl migration with the binding of an additional ligand, L (L = CO, PR_3 , etc.), eq 1. For Na^+

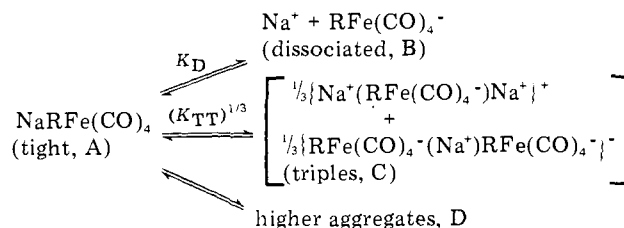


as the counterion and L = PPh_3 , this reaction in THF is slowed 170-fold if the Na^+ is complexed with the crown ether, dicyclohexyl-18-crown-6. Replacement of Na^+ by Li^+ accelerates the alkyl migration. In order to understand this ion-pairing (Lewis acid) catalysis, a knowledge of the ion-pairing⁶ properties of both the alkyl reactant and acyl product of eq 1, $(\text{RFe}(\text{CO})_4)^-$ and $(\text{RC}(\text{O})\text{Fe}(\text{CO})_4)^-$, respectively) was

Scheme I. Synthetic Organic Conversions Using $\text{Na}_2\text{Fe}(\text{CO})_4$



Scheme II. $\text{NaRFe}(\text{CO})_4$ Ion Pairing



required. In general, our studies have focused upon the sodium salt ($\text{NaRFe}(\text{CO})_4$ where $\text{R} = n\text{-C}_{10}\text{H}_{21}$).

Determination of Ion-Pairing Equilibrium Constants Using Conductivity. The concave curve in THF of molar conductance vs. $\text{NaRFe}(\text{CO})_4$ concentration, Figure 1, is typical⁷ of a system that forms ion pairs, dissociated ions, and triple ions in the concentration range studied (A, B, C, respectively, Scheme II).⁸

These conductivity data are most conveniently analyzed⁷ in terms of the following equilibria for ion-pair dissociation, K_D , and the equilibria for triple ion dissociation, K_{TD} . The symbols C , α , and γ_3 have their usual meanings⁷ of the total concentration (e.g., $[\text{NaRFe}(\text{CO})_4]$ total), the degree of dissociation, and the degree of association (of triples), respectively. Analysis⁹ of the conductivity data yields the estimates^{9b} $K_D = 9 \times 10^{-5}$ M and $K_{TD} = 6 \times 10^{-3}$ M (for $\text{R} = n\text{-C}_{10}\text{H}_{21}$ at 25 °C). These equilibrium constants can be used to calculate^{9c} the constant for the total triple ion equilibria (Scheme

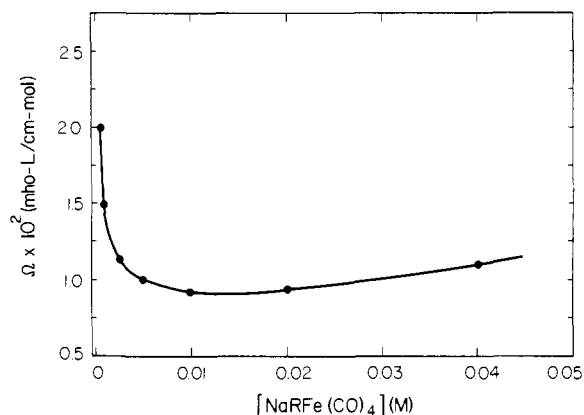


Figure 1. Molar conductance vs. dilution for $NaRFe(CO)_4$ in THF at 25 °C ($R = n-C_{10}H_{21}$).

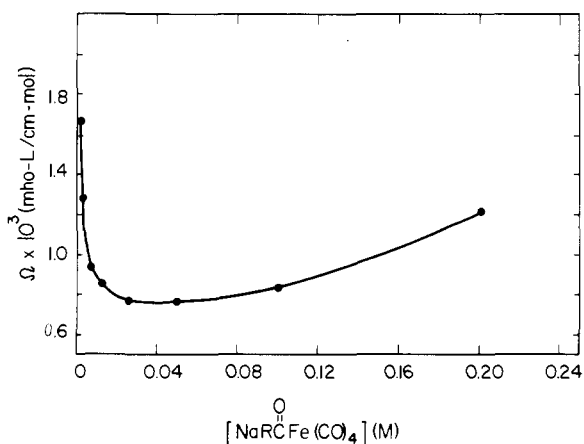
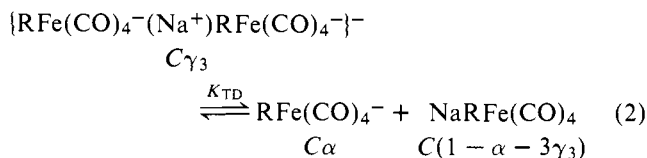
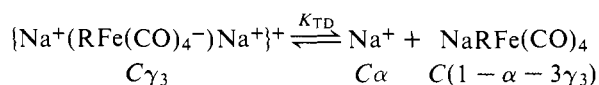
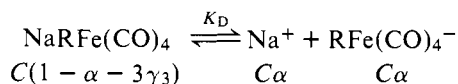


Figure 2. Molar conductance vs. dilution for $NaRC(O)Fe(CO)_4$ in THF at 25 °C ($R = n-C_{10}H_{21}$).

II), $K_{TT} = 2 M^{-1}$. Analysis⁹ of the conductivity data for $NaRC(O)Fe(CO)_4$ (Figure 2) yields the important results that there is significantly tighter cation binding, $K_D = 5 \times 10^{-7} M$, and that there is less tendency to form triple ions, $K_{TD} = 1 \times 10^{-2} M$, $K_{TT} = 5 \times 10^{-3} M^{-1}$. Table I shows relative percentages of the various types of ions at selected concentrations.



Determination of Cation Binding Sites in $RC(O)Fe(CO)_4^-$. Based upon the recent work of Darensbourg^{10b} in different but related systems, there is little doubt that the cation (M^+) in $M^+(RFe(CO)_4^-)$ is associated with the oxygens of the carbonyl groups. More interesting and more pertinent to this work, however, is the cation binding site in $M^+(RC(O)Fe(CO)_4^-)$. Because of the acyl \leftrightarrow oxy carbene resonance structure, we

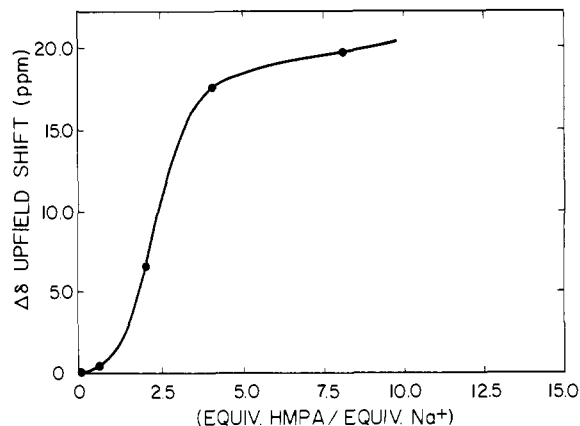


Figure 3. ^{13}C NMR chemical shift of the acyl peak in $NaRC(O)Fe(CO)_4$ ($R = CH_3CH_2$) as a function of added HMPA. $NaRC(O)Fe(CO)_4$ with no HMPA, δ 279.7 ppm downfield from Me_4Si used as a reference ($\Delta\delta = 279.7 - \delta$).

Table I. Relative Percentages of Initial $NaRFe(CO)_4$ or $NaRC(O)Fe(CO)_4$ Present as Ion Pairs, Triple Ions, or Dissociated Ions ($R = n-C_{10}H_{21}$)

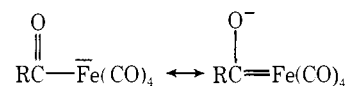
selected initial concn, M	$NaRFe(CO)_4$ or $NaRC(O)Fe(CO)_4$	% triple ^a ions	% ion pairs	% dissociated
2×10^{-1}	alkyl	56	43	1
	acyl	8	91	0.1
5×10^{-2}	alkyl	41	56	3
	acyl	4	95	0.3
1×10^{-3}	alkyl	8	68	24
	acyl	0.6	98	2
1×10^{-5}	alkyl	0.04	9	91
	acyl	0.05	80	20

^a The percent of either $[Na^+(X^-)Na^+]^+$ or $[X^-(Na^+)X^-]^-$ ($X^- = RFe(CO)_4^-$ or $RC(O)Fe(CO)_4^-$) is $1/2$ of this value.

Table II. Cation Dependent Shifts in the Acyl Stretching Frequency in $RC(O)Fe(CO)_4^-$

cation	acyl frequency, cm^{-1}
$(Ph_3P)_2N^+$	1610
Na^+	1585
Li^+	1560

anticipated that the acyl group was the cation binding site in $(RC(O)Fe(CO)_4)^-$. Consistent with this picture, the acyl



stretching frequency (Table II) shifts to lower values with smaller, less polarizable cations such as Li^+ , suggesting increased importance of the oxy carbene resonance structure. Further evidence for the acyl as the cation binding site was obtained using ^{13}C NMR. Although the positions of carbonyl ^{13}C NMR peaks in $(RFe(CO)_4)^-$ and $(RC(O)Fe(CO)_4)^-$ are virtually independent of cation and solvent, the acyl ^{13}C NMR peak of the acyl-iron anion is strongly affected by such changes. The acyl ^{13}C NMR resonance in $(CH_3CH_2C(O)Fe(CO)_4)^-$ is shifted upfield by 19.5 ppm by the addition of a large excess of HMPA (Figure 3). Changing the cation from Na^+ to $(Ph_3P)_2N^+$ causes a shift of 18.2 ppm in the same direction. By comparison, the methyl ^{13}C NMR signal in the propionyl iron complex shows a change of only ~ 0.1 ppm and the carbonyls show a downfield shift of ~ 0.7 ppm. Carbene

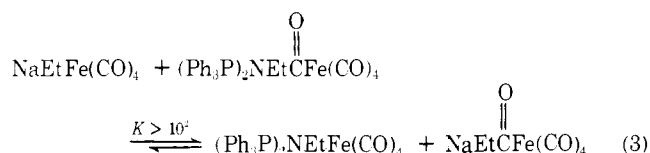
Table III. Selected Equilibrium Constants for Anionic Metal Carbonyl Ion Pairs in THF^a

compd	$K_D \times 10^5$, M	$K_{TD} \times 10^3$, M	ref
Na(NaFe(CO) ₄)	~0.5		4
NaRFe(CO) ₄	9	6	this work
NaRC(O)Fe(CO) ₄	0.05	10	this work
LiMo(CO) ₅ (C(O)Ph)	~0.01		10c
LiMn(CO) ₅	4.3	4.5	10b
NaMn(CO) ₅	2.0	6.4	10b
(Na-crown) ^b Mn(CO) ₅	3.9	5.3	10b
(Ph ₃ P) ₂ N(Co(CO) ₄)	9.4		10d

^a All values at 25 ± 1 °C. ^b Crown = 15-crown-5.

ligands in complexes such as Cr(CO)₅[C(OCH₃)CH₃] (δ 362.3) exhibit¹¹ ¹³C resonances at much lower field than acyl groups as in¹¹ Fe(η⁵-C₅H₅)(CO)₂[C(O)CH₃] (δ 254.4). These ¹³C NMR and IR results provide compelling evidence that the acyl group is the predominant cation binding site in (RC(O)-Fe(CO)₄)⁻.

Several additional general features important to this work can be gleaned from available literature data. The data in Table III clearly indicate that for a variety of cations, metal carbonyl monoanions in THF generally have K_D and K_{TD} values in the range 10⁻⁷-10⁻⁴ (25 °C) and 10⁻³-10⁻², respectively. Tight ion pairs are often present. (At 6.7 × 10⁻³ M, 48% of NaMn(CO)₅ is present as tight ion pairs^{10b}.) The predominant effect of the addition of crown ethers or a few equivalents of dipolar aprotic solvents is to convert contact to solvent-separated ion pairs. In the acyl anions, the preference of the acyl group for small, nonpolarizable cations such as Li⁺ is reflected in their tighter binding (smaller K_D values). The preference of the acyl in (RC(O)Fe(CO)₄)⁻ for Na⁺ rather than the large (Ph₃P)₂N⁺ was confirmed by examining the following equilibrium.



Solutions (0.05 M) of Na(EtFe(CO)₄) and (Ph₃P)₂N(EtC(O)Fe(CO)₄) were mixed and the relative sizes of the acyl peaks at 1585 (Na⁺) and 1610 cm⁻¹ ((Ph₃P)₂N⁺) used to monitor the position of the equilibrium. The estimated equilibrium constant, $K > 10^2$ (eq 3), is predominantly a reflection of the tighter Na⁺ binding by the acyl compound.

Kinetic Studies of (RFe(CO)₄)⁻ Alkyl Migration Reactions. A compilation of our kinetic results is presented in Table IV. In addition to establishing the overall rate law and detailed ion-pairing effects, we have studied a variety of different phosphorus ligands, CO-promoted migrations, the migratory aptitude of *n*-alkyl vs. the electron-withdrawing benzyl group, and the temperature and solvent dependence of the alkyl migration reaction.

The reaction is overall second order, first order each in [NaRFe(CO)₄] and¹² [Ph₃P], with $k_2(\text{obsd}) = 6.2 \pm 0.5 \times 10^{-2} \text{ M}^{-1} \text{ s}^{-1}$ (entries 1-7, Table IV). The rate of alkyl migration varies by about 20-fold over the series (0.0 °C, THF): Ph₃P < (MeO)₃P < *n*-Bu₃P < CO < Ph₂MeP < Et₃P < PhMe₂P < Me₃P (entries 28, 10, 11, 22 (and ref 13), and 12-18, respectively). When this series is compared to either a steric bulk (cone angle)¹⁴ series or to an "electronic" series^{14,15} for the phosphorus ligands, no simple correlation is observed. Thus, as one would expect, both steric and electronic effects seem to influence the relative reactivities of the various phosphorus ligands.

The dramatic effect of ion pairing upon these reactions is evident upon examining Table V. Thus the reaction is slowed by >10³ if the Li⁺ counterion is replaced by (Na-crown)⁺ or (Ph₃P)₂N⁺ and varies Li⁺ > Na⁺ > (Na-crown)⁺ > (Ph₃P)₂N⁺. Since the predominant effect of the addition of crown ether is to convert tight ion pairs to solvent-separated ion pairs, this result and these rate variations (Table V) require that *tight ion paired transition states are much more favorable than are more dissociated ones*. The remaining data (Table IV) show that the apparent activation parameters¹⁶ for this reaction in THF are $\Delta H^\ddagger = 19.3 \pm 0.6 \text{ kcal/mol}$, $\Delta S^\ddagger = -19 \pm 2 \text{ eu}$ (Table IV, entries 25-28), that benzyl migrates roughly¹⁷ 60 times more slowly than *n*-alkyl (entry 29 and ref 17), that the reaction is slowed 35% by addition of 2.4 equiv of H₂O/equiv NaRFe(CO)₄, and that a change in solvent from THF to NMP (*n*-methylpyrrolidinone) slows the reaction 413-fold (33 and 43).

Table IV. Kinetic Data for the Alkyl Migration Reaction:^a M⁺(RFe(CO)₄)⁻ + L → M⁺(RC(=O)Fe(CO)₃L)⁻

entry	L	[L], M	[M ⁺ (RFe(CO) ₄) ⁻], M	Temp, °C	k_2 , ^b M ⁻¹ s ⁻¹	misc exptl info or comment
[NaRFe(CO) ₄] and [PPh ₃] Dependence						
1	Ph ₃ P	0.344	3.3 × 10 ⁻²	25.0	5.8 × 10 ⁻²	
2	Ph ₃ P	0.127	1.64 × 10 ⁻²	25.0	5.6 × 10 ⁻²	
3	Ph ₃ P	0.0668	5.0 × 10 ⁻³	25.0	5.8 × 10 ⁻²	
4	Ph ₃ P	0.0668	2.35 × 10 ⁻³	25.0	6.8 × 10 ⁻²	
5	Ph ₃ P	0.0668	1.12 × 10 ⁻³	25.0	6.3 × 10 ⁻²	
6	Ph ₃ P	0.16	7.3 × 10 ⁻³	25.0	6.1 × 10 ⁻²	
7	Ph ₃ P	0.27	6.6 × 10 ⁻³	25.0	6.7 × 10 ⁻²	
8	Ph ₃ P	0.0668	9.2 × 10 ⁻³	25.0	4.0 × 10 ⁻²	0.022 M degassed H ₂ O added
Reactions with Different Phosphorus Ligands, L						
9	Ph ₂ (CH ₃)P	0.020	4.0 × 10 ⁻³	25.0	22.0 × 10 ⁻²	k_2/k_2^0 (using k_2^0 for PPh ₃ , entry 28)
10	(MeO) ₃ P	0.15	2.5 × 10 ⁻²	0.0	0.35 × 10 ⁻²	1.3
11	<i>n</i> -Bu ₃ P	0.10	2.0 × 10 ⁻²	0.0	0.57 × 10 ⁻²	2.1
12	Ph ₂ MeP	0.25	1.9 × 10 ⁻²	0.0	1.4 × 10 ⁻²	4.8
13	Ph ₂ MeP	0.17	1.7 × 10 ⁻²	0.0	1.2 × 10 ⁻²	
14	Et ₃ P	0.13	2.2 × 10 ⁻²	0.0	1.3 × 10 ⁻²	4.8
15	PhMe ₂ P	0.09	1.7 × 10 ⁻²	0.0	2.8 × 10 ⁻²	10.4
16	Me ₃ P	0.10	2.0 × 10 ⁻²	0.0	4.5 × 10 ⁻²	~20
17	Me ₃ P	0.20	2.5 × 10 ⁻²	0.0	4.6 × 10 ⁻²	
18	Me ₃ P	0.50	2.3 × 10 ⁻²	0.0	5.8 × 10 ⁻²	

Table IV (Continued)

Reactions with CO						
entry	L	CO pressure, atm	$[M^+(RFe(CO)_4)^-]$, ^a M	Temp, °C	k_2 , atm ⁻¹ s ⁻¹	reaction monitored
19	CO	1.0	0.01	25.0	$1.27 \pm 0.07 \times 10^{-3}$ ^d	volumetrically
20	CO	1.0	0.025	25.0	1.3×10^{-3}	IR
21	CO	1.0	0.025	25.0	1.25×10^{-3}	GLC
22	CO	1.0	0.025	0.0	$0.06 \pm 0.004 \times 10^{-3}$ ^d	GLC
23	CO	0.51	0.01	25.0	1.29×10^{-3}	volumetrically
24	CO	0.58	0.01	25.0	1.26×10^{-3}	volumetrically

entry	L	$[L]$ M	$[M^+(RFe(CO)_4)^-]$, M	Temp, °C	k_2 , ^b M ⁻¹ s ⁻¹	misc exptl info or comment
Temperature Dependence ^d						
25	Ph ₃ P	0.0668	9.9×10^{-3}	20.0	3.15×10^{-2}	
26	Ph ₃ P	0.0668	9.6×10^{-3}	14.8	1.64×10^{-2}	
27	Ph ₃ P	0.0668	9.2×10^{-3}	7.90	0.75×10^{-2}	
28	Ph ₃ P	0.0668	8.8×10^{-3}	0.0	0.274×10^{-2}	
Data for Na ⁺ (PhCH ₂ Fe(CO) ₄) ⁻ + PhMe ₂ P ^{c,e}						
29	PhMe ₂ P	0.159	6.2×10^{-3}	25.0	0.105×10^{-2}	
30	PhMe ₂ P	0.325	8.0×10^{-3}	25.0	0.114×10^{-2}	
31	PhMe ₂ P	0.594	6.7×10^{-3}	25.0	0.126×10^{-2}	
32	PhMe ₂ P	1.30	5.6×10^{-3}	25.0	0.159×10^{-2}	
Ion Pairing: Effect of Varying Cation, of Added Crown Ether, of Adding the Polar Solvents HMPA ^f or NMP ^f						
33	Ph ₃ P			25.0	6.2×10^{-2}	average value for M ⁺ = Na ⁺ , entries 1-6
34	Ph ₃ P	0.127	8.7×10^{-3}	25.0	0.036×10^{-2}	0.01 M dicyclohexyl-18-crown-6 (A isomer) added
35	Ph ₃ P	0.20	10.0×10^{-3}	25.0	0.015×10^{-2}	M ⁺ = (Ph ₃ P) ₂ N ⁺
36	Ph ₃ P	0.040	6.0×10^{-3}	25.0	37.0×10^{-2}	M ⁺ = Li ⁺
37	Ph ₃ P	0.067	6.7×10^{-3}	22.5	1.3×10^{-2}	0.013 M HMPA added (2.0 equiv)
38	Ph ₃ P	0.067	6.7×10^{-3}	22.5	0.74×10^{-2}	0.022 M HMPA added (3.3 equiv)
39	Ph ₃ P	0.073	4.5×10^{-3}	22.5	0.13×10^{-2}	0.051 M HMPA added (11 equiv)
40	Ph ₃ P	0.080	3.0×10^{-2}	22.5	0.59×10^{-2}	0.15 M NMP added (5 equiv)
41	Ph ₃ P	0.080	3.0×10^{-2}	22.5	0.23×10^{-2}	0.30 M NMP added (10 equiv)
42	Ph ₃ P	0.080	3.0×10^{-2}	22.5	0.056×10^{-2}	0.50 M NMP added (16 equiv)
Reactions in Pure NMP ^f						
43	Ph ₃ P	1.0	0.10	25.0	0.015×10^{-2}	R = <i>n</i> -C ₅ H ₁₁ used
44	Me ₃ P	<i>g</i>	0.05	25.0	$0.12 \pm 0.01 \times 10^{-2}$ ^g	R = <i>n</i> -C ₅ H ₁₁ used

^a R = either *n*-C₁₀H₂₁- or *n*-C₉H₁₉-, M⁺ = Na⁺, L = PPh₃, in THF unless noted otherwise. ^b $k_2 = k_{1(av)}/[L]$. $k_{1(av)}$ is the average pseudo-first-order rate constants for the disappearance of reactants and appearance of products (measured as RH and RCHO, respectively, after acid quench). ^c Effective NaRFe(CO)₄ concentration (see Experimental Section). ^d Standard deviation of three experiments. ^e Only the disappearance of reactants was monitored. ^f HMPA = hexamethylphosphoric triamide; NMP = *n*-methylpyrrolidinone. ^g Four experiments were performed at (Me₃P) = 0.026, 0.04, 0.05, and 0.07 M. The standard deviation for k_2 is given.

Table V. Effect of Cation for the Reaction

$M^+(RFe(CO)_4)^- + Ph_3P \xrightarrow[25.00^\circ C]{THF} M^+(RCOFe(CO)_3(PPh_3))$			
M ⁺	k_2 (relative) ^a	M ⁺	k_2 (relative) ^a
Li ⁺	1.0×10^3	(Na·11HMPA) ⁺	3.6
Na ⁺	1.7×10^2	(Na-crown) ⁺	1.0
(Na·2HMPA) ⁺	36	(Ph ₃ P) ₂ N ⁺	0.42
(Na·10NMP) ⁺	6.4		

^a Data from entries 33-42, Table IV.

Proposed Mechanism for (RFe(CO)₄)⁻ Alkyl Migration Reactions. We have combined our results with some pertinent literature data in formulating a mechanism for (RFe(CO)₄)⁻ alkyl migration reactions. Since comprehensive reviews of insertion reactions¹⁸ as well as a very recent review¹⁹ of CO insertion reactions are available, we cite only that literature which is relevant to our mechanism. This mechanism (Scheme III) consists of NaRFe(CO)₄ ion pairs in a rapid prior equilibrium with the tight ion-paired coordinatively unsaturated acyl iron tricarbonyl intermediate followed by rate-determining capture by L.

We have observed only overall second-order kinetics ($k_{-3} \gg k_4[L]$, Scheme III) despite the use of very active phosphines

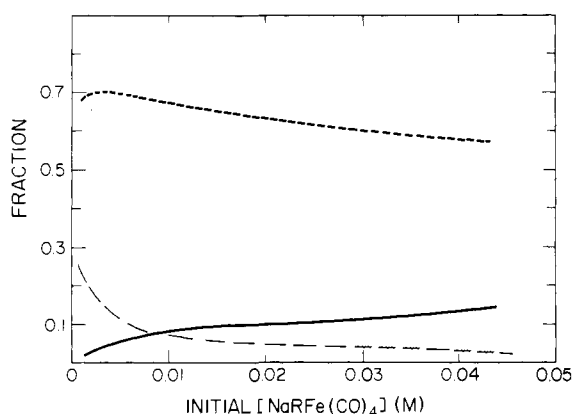
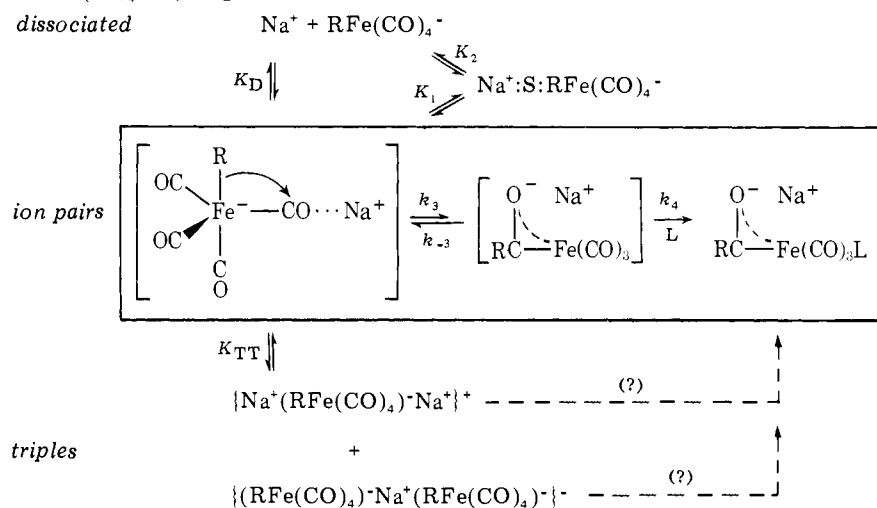
Scheme III. Proposed NaRFe(CO)₄ Alkyl Migration Mechanism

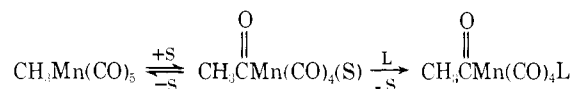
Figure 4. Calculated fraction of ion pairs, triple ions, or dissociated ions present as a function of the initial $[\text{NaRFe}(\text{CO})_4]$. (The — —, indicate the fraction, α , present as dissociated ions; —, the fraction, γ_3 , present as triples; - - -, the fraction, $(1 - \alpha - 3\gamma_3)$, present as ion pairs. The calculation used eq 2, $K_D = 9 \times 10^{-5}$ M, and $K_{TD} = 6 \times 10^{-3}$ M.)

(Table IV, 10–18). Thus we have not been able to obtain the limiting conditions of $k_{-3} \ll k_4[\text{L}]$ to provide kinetic evidence for the proposed prior equilibrium. However, this prior equilibrium has been firmly and widely established in the well-studied $\text{CH}_3\text{Mn}(\text{CO})_5$ system, and our mechanism, therefore, incorporates this feature. The observed ion-pairing effects are nicely accommodated by this prior equilibrium. As a model for ion pairing to the coordinatively unsaturated $\text{RC}(\text{O})\text{Fe}(\text{CO})_3^-$ intermediate, we can use saturated $\text{RC}(\text{O})\text{Fe}(\text{CO})_4^-$. Since the proposed unsaturated intermediate has one less electron-withdrawing CO, it should form even stronger ion pairs than the saturated $\text{RC}(\text{O})\text{Fe}(\text{CO})_4^-$ model. Thus the rate of alkyl migration is dramatically increased by the presence of Lewis acids such as Li^+ because they stabilize the unsaturated $\text{RC}(\text{O})\text{Fe}(\text{CO})_3^-$ intermediate (i.e., increase the equilibrium K_3 , Scheme III) by tight ion pairing to the acyl group.

Although our results imply that solvent-separated or dissociated transition states are less important, we cannot determine whether (tight) triple ions contribute to the overall rate. In principle, it is possible to determine the triples' contribution, although, in practice, it has been done in only a few cases.^{6d,20} Figure 4 gives an indication of how the contributions due to triples (as well as ion pairs and dissociated ions) can be determined. The fraction of triples, ion pairs, and dissociated ions is a function of the initial $[\text{NaRFe}(\text{CO})_4]$. The fraction of these various species over the $\text{NaRFe}(\text{CO})_4$ concentration

range we have studied is presented in Figure 4, and was calculated using the known values of K_D and K_{TD} and the equilibria shown in eq 2. If only ion pairs are reactive, then $k_2(\text{obsd})$ plotted vs. the $[\text{NaRFe}(\text{CO})_4]$ initial should have²¹ the same shape as the calculated concentrations of ion pairs (Figure 4). Similarly, if triples as well as ion pairs are kinetically important, the $k_2(\text{obsd})$ vs. $[\text{NaRFe}(\text{CO})_4]$ initial curve should have²¹ the shape of a weighted sum of the pairs and triples curves (Figure 4). Unfortunately, our experimental $k_2(\text{obsd})$ vs. $[\text{NaRFe}(\text{CO})_4]$ initial data of $\pm 15\%$ precision (entries 1–7, Table IV) are fit equally well by assuming either ion pairs only or pairs plus triples as the kinetically dominant species. Since experimental problems greatly inhibit the use of the optimum $\text{NaRFe}(\text{CO})_4$ concentration ranges,²² the relative contributions of ion pairs vs. (tight) triples cannot be assessed at present. This analysis may be incorrect if the ion pairing characteristics of the transition state are much different from those of the reactant.

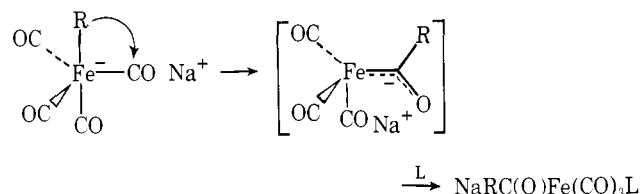
In the alkyl migration reactions of $\text{CH}_3\text{Mn}(\text{CO})_5$, it is well known that polar solvents (S) can participate in the prior equilibrium, acting as transient ligands.¹⁹



Since polar solvents can result in rate increases of 10^3 – 10^4 for $\text{CH}_3\text{Mn}(\text{CO})_5$ migrations,²³ we briefly examined the polar solvent NMP. With $\text{NaRFe}(\text{CO})_4$ migrations, changing from THF to NMP slows the reaction 413-fold, an effect opposite to that generally found in other alkyl migrations. Clearly ion-pairing effects again are dominant. The polar solvent NMP effectively breaks up the tight ion pairs, resulting in the observed rate decrease.

It is also worth mentioning several other aspects of alkyl migrations that may apply to the $\text{NaRFe}(\text{CO})_4$ reactions, Scheme III. We assume that the alkyl group (rather than CO) migrates in $\text{NaRFe}(\text{CO})_4$ as has been demonstrated²⁴ for $\text{CH}_3\text{Mn}(\text{CO})_5$. It is also quite likely that $\text{NaRFe}(\text{CO})_4$ migrations are stereospecific with retention of configuration at carbon. All known alkyl migrations which have been studied with chiral alkyl groups have been shown to proceed with retention at carbon.²⁵ This hypothesis is fortified by our observation that the alkyl ketone synthesis, Scheme I, proceeds cleanly with inversion at carbon^{2b}—undoubtedly via inversion in the $\text{S}_{\text{N}}2$ oxidative-addition step⁴ followed by retention in the alkyl migration step. As indicated in Scheme III, $\text{NaRFe}(\text{CO})_4$ probably has a trigonal bipyramidal structure in solution with the Na^+ coordinated to oxygen^{10b} of an equatorial CO group,

and would, therefore, involve migration of the axial alkyl to an equatorial CO to give $RC(O)Fe(CO)_3^-$. Consistent



with the proposal is a recent x-ray diffraction study²⁶ of $[(\text{Ph}_3\text{P})_2\text{N}](\text{CH}_3\text{CH}_2\text{CH}_2\text{Fe}(\text{CO})_4)$ which shows a trigonal-bipyramidal structure (C_{3v} symmetry) with the alkyl group in the apical position. The pattern of ν_{CO} frequencies in solution²⁷ suggests that this C_{3v} symmetry is also maintained in solution, although the observation of a single ^{13}C NMR signal²⁸ at ambient temperature indicates rapid scrambling of the axial and equatorial groups—a property characteristic of many pentacoordinate complexes.²⁹ The ion pairing of Na^+ with the equatorial rather than axial carbonyls of $RFe(\text{CO})_4^-$ proposed in Scheme III is based on recent work^{10b} demonstrating this mode of ion pairing for $\text{NaMn}(\text{CO})_4(\text{PR}_3)$.

Summary

We have presented evidence for the mechanism of $(RFe(\text{CO})_4)^-$ alkyl migration reactions and have investigated the effect of ion-pairing (Lewis acid) catalysis. Currently we are investigating the importance of ion pairing in a bimetallic system that shows a novel adjacent metal promoted alkyl migration reaction.³⁰

Experimental Section

A. General. 1. Methods for Handling Air-Sensitive Compounds. Air- and water-free conditions were maintained at all times throughout this work. The techniques used have been previously described in detail.⁴

2. Equipment. IR and 60-MHz NMR spectra, gas-liquid chromatography, conductivity measurements, and temperature control were accomplished using the same equipment previously described.⁴ Quantification for gas-liquid chromatography was accomplished using a Vidar 6300 digital integrator. A Varian XL-100 pulsed Fourier transform nuclear magnetic resonance spectrometer was used to record ^{13}C NMR spectra.

B. Materials. 1. General. $\text{Fe}(\text{CO})_5$ (Pressure Chemical Co.) was filtered and stored in a dark bottle over Linde 4A sieves under nitrogen. Sodium dispersion (50% in paraffin) was obtained from Matheson Coleman and Bell Chemical Co. The outer layer was scraped off and the inner part was used. Bis(triphenylphosphine)iminium chloride $[(\text{Ph}_3\text{P})_2\text{N}^+\text{Cl}^-]$ was prepared by the method of Ruff,³¹ recrystallized from water, and dried using an Abderhalden. Gases were purchased from the Liquid Carbonic Corp. Nitrogen (99.996%) was further purified by passage through a BASF oxygen scavenger and Linde 3A molecular sieve. Carbon monoxide (99.2%) contained nitrogen (0.7%) as its principal impurity; it contained less than 0.05% oxygen and water. The solvents THF, NMP, and HMPA were all dried and distilled as outlined before.⁴ Alkyl halides (Aldrich) were distilled from P_2O_5 under nitrogen prior to use and stored in a dark bottle. Dicyclohexyl-18-crown-6 crown ether (Aldrich technical grade—received as an impure mixture of A and B isomers) was purified by chromatography on neutral alumina (eluting with an Et_2O -hexane mixture). Only the A isomer, mp 60.0–62.0 °C (lit. 61–62.5 °C), was used. A better method for the purification of dicyclohexyl-18-crown-6 has since been reported.

2. $\text{Na}_2\text{Fe}(\text{CO})_4$. A procedure for the preparation of $\text{Na}_2\text{Fe}(\text{CO})_4$ has been published.⁴

3. Preparation of Anhydrous Lithium Bromide. Anhydrous lithium bromide was prepared from lithium ribbon and 1,2-dibromoethane in dry THF under nitrogen. After benzene was added and the solution was concentrated, the resulting white crystals were filtered using Schlenk tube techniques, washed with dry hexane, dried overnight, and then stored in a Vacuum Atmospheres drybox.

4. Standard Procedure for Preparing THF Solutions of Sodium Decyltetracarbonylferrate(0). As a typical example, in the drybox 108

mg of $\text{Na}_2\text{Fe}(\text{CO})_4$, a small stir bar, 50 mL of dry THF, 115 μL of *n*-decyl bromide (10% excess), and 50 μL of *n*-undecane as an internal standard were added to a clean, dry centrifuge tube. After a new, tightly fitting septum cap was inserted, folded over, and taped in place with black electrical tape, the centrifuge tube was removed from the box and stirred for roughly 0.5 h at 0 °C. This solution was either centrifuged or allowed to settle overnight at –22 °C to remove the colloidal NaBr. The resulting clear, light tan solution was then ready for use. Any solutions darker than light tan were discarded.

5. Preparation of Solutions of $\text{M}^+[\text{RFe}(\text{CO})_4]^-$ ($\text{M}^+ = \text{Li}^+$, $(\text{PH}_3)_2\text{N}^+$, or $(\text{Na}^+\text{-crown})$). A standard $\text{NaRFe}(\text{CO})_4$ solution, prepared as in 4, was converted to a solution of the Li^+ or $(\text{PPh}_3)_2\text{N}^+$ salt by the following exchange procedure. A slight excess of anhydrous LiBr or $(\text{PPh}_3)_2\text{NCl}$ was weighed into a dry, clean centrifuge tube in the drybox. After a small stir bar was added, the centrifuge tube was capped with a tightly fitting septum which was folded over and taped in place with black electrical tape. This tube was removed from the drybox and the homogeneous contents of a standard $\text{NaRFe}(\text{CO})_4$ solution were anaerobically transferred onto the LiBr or $(\text{PPh}_3)_2\text{NCl}$ using needlestock techniques. After stirring at 0 °C for 1 h, the resulting precipitate of NaCl or NaBr was centrifuged off, and the solution was ready for use. $(\text{Na}^+\text{-crown})\text{RFe}(\text{CO})_4$ solutions were made in a similar manner by transferring the homogeneous contents of a standard $\text{NaRFe}(\text{CO})_4$ solution into a nitrogen-filled septum-capped centrifuge tube containing 1 equiv of dicyclohexyl-18-crown 6 (A isomer).

6. Phosphines and Phosphites. Caution. Since the most of these are volatile, toxic, and noxious liquids, all operations should be done in a good hood and rubber gloves should be worn. Air-free techniques are required to prevent oxidation of these reagents.

$(\text{CH}_3)_2\text{PhP}$ (M and T Chemicals) was distilled at reduced pressure and stored under nitrogen in a hood. $(\text{CH}_3)_3\text{P}$ was prepared by the method of Thomas and Eriks.³³ It was isolated in the pure state in a (–78 °C) trap rather than as the $(\text{CH}_3)_3\text{P-AgI}$ complex.

$(\text{CH}_3)_3\text{P}$ was prepared by addition of methylmagnesium chloride (3 M in THF, M and T Chemicals) to chlorodiphenylphosphine (Aldrich) in THF. After a quench with cold, saturated ammonium chloride solution, the mixture was extracted with ether, washed with water and salt solution, dried, and distilled (100–105 °C, 0.15 mm), yield 72%.

The following were used as received: *n*- Bu_3P (Strem), Et_3P (Strem), and $(\text{MeO})_3\text{P}$ (MCB).

Ph_3P (MCB) was recrystallized from ethanol and dried using an Abderhalden.

C. Kinetics. 1. The reaction of $\text{NaRFe}(\text{CO})_4$ with Ph_3P in THF will be described in detail as an example of the general procedure used. The kinetic experiments were carried out using one vial for each kinetic point.

In a typical run, the light tan $\text{Na}[n\text{-C}_{10}\text{H}_{21}\text{Fe}(\text{CO})_4]$ solution prepared as in (B-4) was transferred back into the drybox and 2 mL was transferred into each of eight clean, dry, two-dram vials. After each was capped with a tight fitting septum, they were removed from the box, suspended in a constant-temperature bath, and allowed to come to thermal equilibrium. The reaction was started by injection (via gas-tight syringe) of a stock solution of Ph_3P in THF with vigorous swirling to ensure good mixing. In all cases, except those specifically noted, the conditions were pseudo-first-order with phosphine in excess. At the end of the measured time intervals, the reaction in each vial was quenched by the injection of a two- to tenfold excess of glacial acetic acid or concentrated hydrochloric acid. The quench times were chosen to cover a range from 10 to 75% reaction, as well as zero and infinity (10 half-lives). The quench formed decane (as a measure of reactants, $\text{Na}[n\text{-C}_{10}\text{H}_{21}\text{Fe}(\text{CO})_4]$) and undecanal (as a measure of the products, $\text{Na}[n\text{-C}_{10}\text{H}_{21}\text{C}(\text{O})\text{Fe}(\text{CO})_4]$) which were simultaneously assayed by GLC using the internal standard undecane. The crude, quenched reaction mixture was injected directly in the GLC without workup. After analysis of the data, this procedure gives two values of the rate constant (k (reactants) and k (products)) for each run.

2. Determination of Effective $[\text{NaRFe}(\text{CO})_4]$. In general, since the reactions were run under pseudo-first-order conditions with phosphine in excess, it was not necessary to precisely know the active $\text{NaRFe}(\text{CO})_4$ concentration. However, especially in entries 1–8, Table IV, it was necessary to get a better estimate of the active $\text{NaRFe}(\text{CO})_4$ concentration in order to possibly evaluate the different rate contributions due to ion pairs, dissociated ions, and triple ions (see the

Discussion section). The effective $[\text{NaRFe}(\text{CO})_4]$ was evaluated as follows:

$$[\text{NaRFe}(\text{CO})_4]_{\text{effective}} = (\text{M internal standard}) \left(\frac{\text{area product}}{\text{area standard}} \right) \times (\text{GLC response correction factor})$$

3. Volumetric Procedure for Measuring the Rates of Reactions with CO. The gas volumetric apparatus used was a simple version of the one described by Calderazzo and Cotton.³⁴ It consisted of a 60-mL buret (graduated to 0.2 mL) connected at the top via a Teflon gas valve and capillary tubing to a three-neck, 100-mL round-bottom flask which contained a stir bar. A manometer attached to the top side of the buret and a mercury leveling bulb attached to the bottom of the buret completed the device. The flask was thermostated using a water bath. Reactions were initiated by adding a standard $\text{NaRFe}(\text{CO})_4$ solution to the CO filled apparatus. By using the leveling bulb to keep the manometer close to level throughout the run, a constant CO pressure was maintained and the volume of CO consumed was followed as a function of time.

4. Reactions with CO Followed by GLC and IR. These reactions were followed by removing aliquots from a reaction flask and either quenching them with acid and doing a GLC analysis or using their infrared spectrum in the carbonyl region, following the loss in absorbance of the alkyltetracarbonylferate peak at 1833 cm^{-1} and the gain of the acyltetracarbonyl peak at 1925 cm^{-1} .

5. Analysis of the Kinetic Data. In general, the kinetic studies were run under pseudo-first-order conditions and both the concentration of reactants and products were simultaneously monitored giving two values for the pseudo-first-order rate constant, k_1 , in each run. These rate constants were found as previously published⁴ using the first-order integrated rate equation and least-squares methods.

D. Conductance vs. Dilution Experiments. These experiments were performed in the drybox at $25 \pm 2 \text{ }^\circ\text{C}$, with the conductivity cell connected via wire leads to a bridge outside the drybox. Using extra care to avoid adventitious H_2O , six or seven serial dilutions of the original $\text{NaRFe}(\text{CO})_4$ or $\text{NaRC}(\text{O})\text{Fe}(\text{CO})_4$ were made in the drybox. Starting with the most dilute solution, the conductance at each dilution was measured.

E. ^{13}C NMR Spectra. For maximum sensitivity, concentrated solutions (0.1–0.5 M) and 12-mm sample tubes were used. The acyl and iron carbonyl ^{13}C NMR peaks saturate easily requiring the use of short, 15–30 μs , pulse widths. Me_4Si was used as an internal standard and benzene- d_6 for the deuterium lock.

Acknowledgment. We thank Dr. S. Winter for his NMR analysis and results which are cited in Figure 3. This work was supported by National Science Foundation Grant CHE75-17018.

References and Notes

- To whom correspondence should be addressed.
- (a) M. P. Cooke, *J. Am. Chem. Soc.*, **92**, 6080 (1970); (b) J. P. Collman, S. R. Winter, and D. R. Clark, *ibid.*, **94**, 1788 (1972); (c) J. P. Collman, S. R. Winter, and R. G. Komoto, *ibid.*, **95**, 249 (1973); (d) J. P. Collman, *Acc. Chem. Res.*, **8**, 342 (1975).
- The term "insertion" is a historical misnomer, since it is now known that, in at least one case and presumably in others, the alkyl group migrates to CO rather than coordinated CO inserting into the metal alkyl bond.
- J. P. Collman, R. G. Finke, J. N. Cawse, and J. I. Brauman, *J. Am. Chem. Soc.*, **99**, 2515 (1977).
- J. P. Collman, J. N. Cawse, and J. I. Brauman, *J. Am. Chem. Soc.*, **94**, 5905 (1972).
- For an introduction to ion pairing see (a) M. Szwarc, "Ions and Ion Pairs in Organic Reactions", Vol. II, Wiley, New York, N.Y., 1974; (b) *ibid.*, Vol. I, 1972; (c) *ibid.*, Vol. I, 1972, p 165; (d) *ibid.*, Vol. II, 1974, p 410.
- (a) R. M. Fuoss and F. Accascina, "Electrolytic Conductance", Interscience, New York, N.Y., 1959, Chapter 18.
- The statement in our original communication⁵ that only tight ion pairs were present is incorrect.
- (a) It can be shown that⁷ for conditions where few triple or dissociated ions are present relative to ion pairs:

$$\Omega C^{1/2} = \Omega_0(K_D)^{1/2} + \lambda_0(C)(K_D)^{1/2}/K_{TD}$$
- where C = initial concentration, and Ω_0 and λ_0 = molar conductivities at infinite dilution of dissociated and triple ions, respectively. Thus from a plot of $\Omega C^{1/2}$ vs. C and given Ω_0 and λ_0 , K_{TD} and K_D can be determined. A value of Ω_0 equal to 0.09 mho/M-cm and the usual assumption⁷ $\lambda_0 = 1/3\Omega_0$ have been used. (b) These estimates are probably within a factor of 2 of their true value. The major error is in the estimation of Ω_0 (and thus λ_0). However, the value $\Omega_0 = 0.09 \text{ mho/M-cm}$ used for both $\text{Na}^+ + \text{RFe}(\text{CO})_4^-$ and $\text{Na}^+ + \text{R}(\text{C}=\text{O})\text{Fe}(\text{CO})_4^-$ in THF is supported by the known values (compound, Ω_0 in parentheses) (THF): NaBPh_4 (0.088),^{10a} $\text{NaCo}(\text{CO})_4$ ^{6c} (0.11), $\text{NaMn}(\text{CO})_5$ (0.13),^{10b} $\text{NaMn}(\text{CO})_4\text{P}(\text{O})\text{Ph}_2$ (0.093). Our treatment of the conductivity data^{9a} neglects effects due to activity coefficients and mobility corrections. It also makes the usual⁷ but untested assumption that K_{TD} is the same for both cationic and anionic triple ions. Finally, K_D and K_{TD} are composite equilibrium constants because of the presence of solvent-separated ion pairs. For example, $K_D = K_1K_2/(1 + K_1)$, where

$$\text{NaRFe}(\text{CO})_4 \xrightleftharpoons{K_1} \text{Na}^+ : \text{S:RFe}(\text{CO})_4^- \quad (\text{S} = \text{solvent})$$

$$\text{Na}^+ : \text{S:RFe}(\text{CO})_4^- \xrightleftharpoons{K_2} \text{Na}^+ + \text{RFe}(\text{CO})_4^-$$
- (c) $K_{TT} = K_D/(K_{TD})^2$.
- (10) (a) J. Smid and M. Szwarc, *J. Phys. Chem.*, **69**, 608 (1965); (b) M. Y. Darensbourg, D. J. Darensbourg, D. Burns, and D. A. Drew, *J. Am. Chem. Soc.*, **98**, 3127 (1976); (c) M. Y. Darensbourg and C. Borman, *Inorg. Chem.*, **15**, 3121 (1976); (d) M. Y. Darensbourg, H. Barros, and L. Borman, *J. Am. Chem. Soc.*, **99**, 1647 (1977).
- (11) L. F. Farnell, E. W. Randall, and E. Rosenberg, *Chem. Commun.*, 1078 (1971).
- (12) In $k_1(\text{obsd})$ vs. $[\text{L}]$ plots some concave curvature was often observed at very high $[\text{L}]$ (for example, see Table IV, entries 16–18 and 29–32). Although these data were better fit by a $[\text{L}]^1$ rather than a $[\text{L}]^{3/2}$ dependence, they are not completely understood at present.
- (13) (a) The concentration of CO in THF at 1.0 atm and $20 \text{ }^\circ\text{C}$ is approximately 0.01 M ;^{13b} thus $k_2 = 7.6 \times 10^{-5} \text{ atm}^{-1} \text{ s}^{-1}$ can be converted to $k_2 = 7.6 \times 10^{-3} \text{ M}^{-1} \text{ s}^{-1}$. (b) J. O. Osburn and P. L. Markovic, *Chem. Eng. (N. Y.)*, **76**, 105 (1969).
- (14) C. A. Tolman, *Chem. Rev.*, **77**, 313 (1977).
- (15) C. A. Tolman, *J. Am. Chem. Soc.*, **92**, 2953 (1970).
- (16) Error bars represent one standard deviation from the least-squares analysis; the experimental errors are likely to be larger. These activation parameters are composite values since they include terms from the ion-pairing equilibria. The $\Delta S^\ddagger = -2 \text{ eu}$ we reported earlier^{2d} is in error.
- (17) Using entry 15, Table IV, and the assumption that the alkyl migration reaction for $\text{L} = \text{Ph}_2\text{MeP}$ has roughly the same temperature dependence as we found for $\text{L} = \text{PPh}_3$, we have calculated $k_2(\text{calcd}) \approx 6 \times 10^{-3} \text{ M}^{-1} \text{ s}^{-1}$ for $\text{L} = \text{Ph}_2\text{MeP}$ at $25 \text{ }^\circ\text{C}$.
- (18) A. Wojcicki, *Adv. Organomet. Chem.*, **11**, 87 (1973), and references cited therein.
- (19) F. Calderazzo, *Angew. Chem., Int. Ed. Engl.*, **16**, 299 (1977), and references cited therein.
- (20) (a) K. Takaya and N. Ise, *J. Chem. Soc., Faraday Trans. 1*, **70**, 1338 (1974); (b) K. Takaya, S. Yamauchi, and N. Ise, *ibid.*, **70**, 1330 (1974).
- (21) If only tights are reactive then $k_2(\text{obsd})$ will be given by

$$k_2(\text{obsd}) = k_{2\pm} [\text{tights}] = k_{2\pm} (1 - \alpha - 3\gamma_3)$$
- where $k_{2\pm} = k_3k_4/(k_{-3} + k_4[\text{L}])$, Scheme III. If triples as well as tights are reactive, then $k_2(\text{obsd})$ will be given by

$$k_2(\text{obsd}) = k_{2\pm} [\text{tights}] + k_{2T} [\text{triples}] = k_{2\pm} (1 - \alpha - 3\gamma_3) + k_{2T} \gamma_3$$
- where k_{2T} is the triple-ion rate constant. Note that k_{2T} would probably be a composite constant, since it is likely that the cationic triples, $[\text{Na}^+(\text{RFe}(\text{CO})_4)^-\text{Na}^+]^+$, are more reactive than the anionic ones, $[\{\text{RFe}(\text{CO})_4\}^-\text{Na}^+(\text{RFe}(\text{CO})_4)^-\}]^-$.
- (22) Figure 4 suggests that especially a higher and possibly a lower $\text{NaRFe}(\text{CO})_4$ concentration range than the one employed would be more informative. Unfortunately, more concentrated solutions at $25 \text{ }^\circ\text{C}$ are precluded since $\text{NaRFe}(\text{CO})_4$ rapidly decomposes in concentrated solutions and above $0 \text{ }^\circ\text{C}$. (See footnote 18 in ref 4.) (It may be possible, however, to study more concentrated solutions below $0 \text{ }^\circ\text{C}$.) Lower concentration ranges will be very difficult to study since we have shown that trace amounts of H_2O inhibit the migration reaction (entry 8, Table IV).
- (23) (a) F. Calderazzo and F. A. Cotton, *Inorg. Chem.*, **1**, 30 (1962); (b) R. J. Mawby, F. Basolo, and R. G. Pearson, *J. Am. Chem. Soc.*, **86**, 3394 (1964); (c) K. Noack, M. Ruch, and F. Calderazzo, *Inorg. Chem.*, **7**, 345 (1968).
- (24) K. Noack and F. Calderazzo, *J. Organomet. Chem.*, **10**, 101 (1967).
- (25) P. L. Bock, D. J. Boschetto, J. R. Rasmussen, J. P. Demers, and G. M. Whitesides, *J. Am. Chem. Soc.*, **96**, 2814 (1974).
- (26) G. Huttner and W. Gartztk, *Chem. Ber.*, **108**, 1372 (1975).
- (27) W. O. Siegl and J. P. Collman, *J. Am. Chem. Soc.*, **94**, 2516 (1972).
- (28) S. R. Winter, Ph.D. Thesis, Stanford University, Stanford, Calif., 1973.
- (29) J. R. Shapley and J. A. Osborn, *Acc. Chem. Res.*, **6**, 305 (1973), and references cited therein.
- (30) J. P. Collman, R. K. Rothrock, R. G. Finke, and F. Rose-Munch, *J. Am. Chem. Soc.*, **99**, 7381 (1977).
- (31) J. K. Ruff and W. J. Schlientz, *Inorg. Synth.*, **15**, 84 (1974).
- (32) R. M. Izatt, B. L. Haymore, J. S. Bradshaw, and J. J. Christensen, *Inorg. Chem.*, **14**, 3132 (1975).
- (33) R. Thomas and K. Eriks, *Inorg. Synth.*, **9**, 59 (1967).
- (34) F. Calderazzo and F. A. Cotton, *Inorg. Chem.*, **1**, 30 (1962).